10.21611/qirt.2016.107

Evaluation of respiration rate and pattern using a portable thermal camera

by J. Rumiński*

* Gdansk University of Technology, Narutowicza 11/12, 80-233 Gdansk, Poland, *jacek.ruminski@pg.gda.pl*

Abstract

The goal of this paper was to analyze the accuracy of the proposed method for the evaluation of respiration rate and respiration rhythm patterns (e.g. inspiration slope) using the portable and mobile thermal camera module that could be a part of smart glasses. Parameters were analyzed for 12 volunteers in two experiments, when subjects speak and do not speak. The pressure, chest belt was used as a reference measurement method. Data analysis showed that respiration rate and some respiration-related parameters could be accurately measured with the used methodology.

1. Introduction and related work

Respiratory rate (RR) is one of the vital signs and is defined as the number of breaths per minute. Evaluation of respiratory rate values is used to classify if respirations are normal, too fast (tachypnea), too slow (bradypnea), or nonexistent (apnea). In clinical observations, the respiratory rate is often measured by counting the number of times the chest rises or falls per minute [1]. It is important parameter indicating potential health risks, for example, it could be a predictor of cardiac problems (e.g. when RR> 27bpm [2]); pneumonia [3][4] or lower respiratory tract infection [5]. It was also recommended to accurately measure respiratory rate at least once a day for patients in hospitals and during admission to hospitals [6].

In literature, there are many automatic and quantitative methods of RR measurement proposed, for example, using inductive plethysmographs or thoracic impedance systems [7], oxygen masks [8], bioacoustics sensors [9], accelerometers or gyroscope sensors [10], cameras, etc. Often, as for analysis of quality of sleep, respiratory rate is measured together with other biomedical signals like electroencephalogram, electro-oculogram, electromyogram, nasal airflow, abdominal and/or thoracic movements, body position, snore acoustic signal, electrocardiogram, and blood oxygen saturation [11][12].

In some applications (e.g. severe acute respiratory syndrome - SARS, pandemic influenza, etc.) remote measurement of respiration rate could be very important. Therefore the use of visible light, near infrared and thermal imaging was found as useful methods for the evaluation of chest respiration movements or nasal heat flow. In [13] near infrared illumination module and a camera module were used as an active-stereo depth-sensing system. Depth map was used to detect volumes of potential respiratory-related movements (the rib cage and the abdominal cavity) and next breathing signals were extracted from a set of frames. However, in this method it is required to wear tight, elastic tops during measurements. Extraction of signals from a series of thermal images has been previously used to specify diagnostic parameters [14][15]. Thermal, facial videos were analyzed to estimate respiratory rates in [16][17]. Methods presented in [18][19] allow extracting respiration waveforms from registration of heat transfer of the moisturized air during expiration. The side- view of the subject to the camera is used, in order to visualize breathing-jet dynamics. For the presented measurement methods RR was typically estimated using statistical methods or using analysis of dominating peaks in the frequency spectrum. In [20] temperature gradient distribution throughout the nasal cavity was used to extract respiration waveforms. The authors compared results of their method with manually registered values from the reference bedside monitor. The validation was performed for 5 subjects and showed small differences between the estimated values using the thermal-based method and the reference values (mean=1.18bpm, std. dev.=0.80).

The goal of this paper is to analyze the accuracy of the proposed method for the evaluation of respiration rate and respiration rhythm patterns using the portable and mobile thermal camera module that could be a part of smart glasses. Additionally, it was important to evaluate methods of respiration rate estimation for two conditions: a subject is silent and a subject speaks during the measurement. The practical objective is to analyze if a physician (e.g. specializing in treatment of allergies) could estimate respiration parameters during routine interview (e.g. when a patient describing his/her problem).

2. Methodology

Under the eGlasses project we are developing the smart glasses platform that can use different sensors, including visible and thermal cameras. The TAMARISK 320 thermal camera (Fig. 1, left) was used in this study to record thermal images (resolution 320x240. sensitivity<50mK. spectral band: 8-14um).

It was assumed that due to respiration activities temperature is changing in the region of the nose or/and mouth. For each video frame the region of interest (ROI) is extracted (e.g. nose area) and corresponding values are averaged (one value for a frame):

$$\bar{s}(t_i) = \frac{1}{N_{ROI}} \sum_{x=C_s}^{C_e} \sum_{y=r_s}^{r_e} T(x,y)$$

where: N_{ROI} - number of pixels in the nose ROI, r_s, c_s - first (start) row and column of the ROI rectangle, r_e, c_e – last (end) row and column of the ROI rectangle, $T(x, y)$ – pixel value of the data matrix of the ROI.

Finally the set of digital values (digital signal) are calculated and normalized to the mean value:

$$\bar{s_n}(t_i) = \bar{s}(t_i) - \mu(\bar{s}(t)).$$

Two experiments were performed. During the first one, 12 healthy volunteers (avg. age = 36.25y±12.08) were asked to sit in the front of the thermal camera and breath without speaking or moving. In the second experiment the same subjects were asked to continuously speak (small head movements were allowed). The respiration belt (Vernier RMB) was used to measure reference respiration signals. The acquisition time was set to 1 minute (sampling frequency for both devices set to 25Hz). All measurements were taken from the distance between 40-70cm. To synchronize both respiration signals subject were asked to hold a breath and start normal breathing 3s-7s after the acquisition had started. Half of experiments took place in the room with ambient temperature set to 22C, other half for temperature 27C.

Data were processed using software designed and implemented in Java programming language and using Octave. The following data pre-processing methods were used for thermal sequences: manual ROI extraction for nose and mouth regions (different size to analyze ROI size influence), high pass filtration using the designed Butterworth filter (*fc*=0.12Hz), moving average filtration (kernel size=FPS*0.4), multiplication by -1 (to synchronize with reference pressure signal). Then the respiration rate was estimated using three methods: the frequency value for the maximum peak in the estimated PSD (labeled as *eRR_sp*), zero-crossing analysis in time domain (*eRR_zc*), inhalation events detection and counting. The algorithm was designed to detect dominated slopes in the signal and related inspiration start/stop events. It is based on the successive accumulation of data points (from a local signal minimum, SI_{min} in t_{min} – inhalation start; to a local signal maximum, SI_{max} in t_{max} – inhalation end) until the approximated first derivative is equal or lower than zero. The difference between the local maximum and minimum was then compared to the experimentally chosen threshold value (0.33*(*globalMax-globalMin*)). Inspiration-related slopes (*S*) were calculated as $acos(C(t_{max}-t_{min})/(SI_{max}-SI_{min}))$, *C*-normalization factor. Expiration time, *Et*, was defined as a time period between t_{max} (current end of inspiration) and the next t_{min} (next start of inspiration). All values were calculated for signals measured using the belt (e.g. *IBt*) and the thermal camera (e.g. *ITt*). Parameters calculated from thermal camera signals were compared to parameters obtained for the belt. For example:

$$\Delta It = |IBt - ITt|,\ \Delta Et = |EBt - ETt|,\ \Delta S = |SB - ST|$$

and normalized to reference values obtained for the belt (*ΔIt/IBt*, *ΔEt/EBt*).

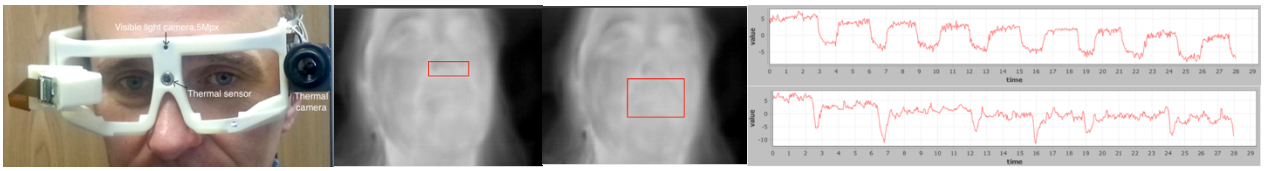

Fig. 1. *From left: The eGlasses prototype with the connected thermal camera, a frame with the nostril ROI, a frame with the mouth ROI, raw signal from the nostril ROI (top), raw signal from the mouth ROI (bottom – speaking experiment)*

Analyzing respiratory waveforms during speaking is much more difficult since extracted signals are more noisy and irregular. Therefore in this study we did not analyze morphological patterns of the extracted signals (e.g. ΔIt, ΔEt, S) but we analyzed different respiratory rate estimators. Apart from previously used methods (*eRR_zc* and *eRR_sp*) we additionally used an estimator based on periodicity of peaks locations for the autocorrelation signal generated as a autocorrelation in a function of time lags. The autocorrelation sequence of a periodic signal has the same cyclic characteristics as the signal itself. Therefore for the *eRR_ac* estimator the autocorrelation for different time lags is calculated and the periodicity is determined calculating an average time differences between detected peaks. Additionally, respiration rate was calculated manually (*RR*) as a number of whole respiration events (inspiration-to-inspiration) in given time window.

3. Results

Examples of respiration rhythm signals measured using the described method for the first experiment (i.e. subjects do not speak) are presented in Fig. 2 (left). Positive slopes represent inhalation. In Table 1 some results for the experiment 1 are presented.

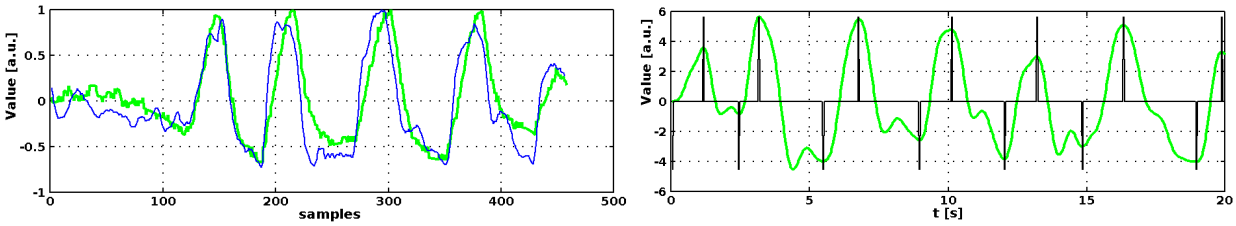

Fig. 2. *From left: respiration signals (blue: thermal camera, green: belt); detection of inhalation/exhalation events*

Table 1. *The results for the experiment 1 (without speaking)*

Subject	***eRR_zc* (belt)**	***eRR_zc* (thermal)**	***eRR_sp* (belt)**	***eRR_sp* (thermal)**	**ΔIt/IBt**	**ΔEt/EBt**	**ΔS**
	bpm	**bpm**	**bpm**	**bpm**	**%**	**%**	**degrees**
S01	19.85	19.85	17.58	17.58	25.22	17.43	3.43
S02	10.50	10.50	8.79	8.79	29.70	17.89	5.56
S03	9.64	9.64	8.79	8.79	38.40	36.50	13.08
S04	18.19	19.29	20.51	20.51	15.03	20.45	0.97
S05	14.03	14.03	14.65	14.65	7.78	3.60	1.45
S06	11.65	11.65	11.72	11.72	12.93	2.63	2.81
S07	13.47	13.47	14.65	14.65	16.52	8.58	2.59
S08	8.75	10.00	11.72	11.72	30.11	10.81	18.32
S09	13.50	13.50	11.72	11.72	15.31	12.38	3.07
S10	10.10	10.10	11.72	11.72	19.53	17.67	3.25
S11	15.00	15.00	14.65	14.65	13.20	28.06	4.13
S12	18.75	20.19	20.51	20.51	6.32	8.78	1.87
Mean	*13.62*	*13.94*	*13.92*	*13.92*	*19.17*	*15.40*	*5.04*
Std. dev.	*3.74*	*3.93*	*3.98*	*3.98*	*9.75*	*9.86*	*5.24*

Results obtained for the experiment 2 (subjects were speaking) were not so good as for the experiment 1. However, inhalation events were visible and relatively easy to detect. In Fig. 3 some signal examples are presented. It is important to underline that irregularities were observed in signals extracted from thermal frames as well as in signals measured using pressure, chest belt.

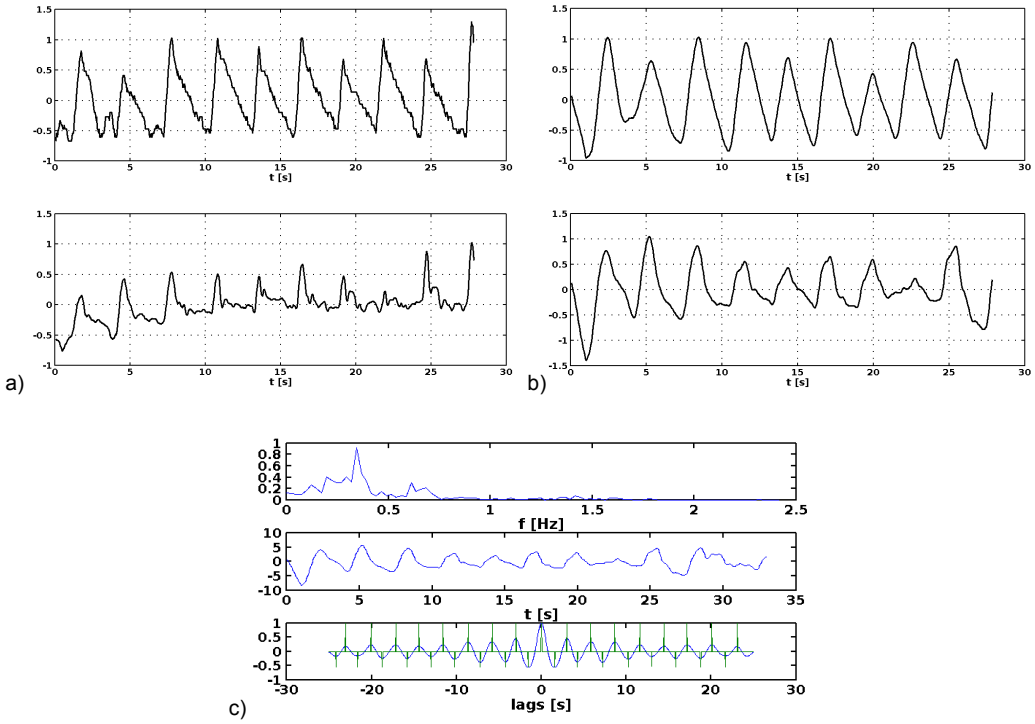

Fig. 3. *Examples of normalized respiratory waveforms. a) Original waveforms for the belt (top) and for thermal camera. b) Filtered signals from a). c) Processed filtered signals: normalized amplitudes in frequency domain (top), autocorrelation as a function of time lags with detected peaks (bottom).*

In Table 2 results for the experiment 2 are presented.

Table 2. *The results for the experiment 2 (speaking)*

	Belt				Thermal camera		
Subject	***RR***	***eRR_zc***	***eRR_sp***	***eRR_ac***	***eRR_zc***	***eRR_sp***	***eRR_ac***
S01	22.00	21.00	24.00	23.08	20.00	22.00	22.58
S02	16.00	15.00	15.00	16.71	15.00	18.00	17.91
S03	11.00	10.97	9.97	10.40	12.97	9.97	10.70
S04	15.00	13.98	15.98	16.01	14.98	9.99	15.46
S05	8.00	10.99	9.99	12.07	14.98	13.98	7.44
S06	16.00	16.98	19.97	10.04	17.98	9.99	14.98
S07	13.00	12.98	15.98	16.01	19.97	11.98	13.84
S08	19.00	17.98	19.97	20.69	18.97	19.97	20.80
S09	7.00	8.99	9.99	10.39	14.98	9.99	6.85
S10	14.00	14.98	9.99	12.74	18.97	13.98	13.71
S11	18.00	12.98	9.99	10.25	11.98	17.98	17.24
S12	14.00	12.98	13.98	13.89	16.98	13.98	13.94

The Root Mean Square Error (RMSE) was calculated between manually calculated *RR* values and automatically calculated values using all estimators. Results are presented in Table 3.

Table 3. *RMSE values calculated for the results of the experiment 2 (speaking)*

	Belt			Thermal camera		
	eRR_zc	***eRR_sp***	***eRR_ac***	***eRR_zc***	***eRR_sp***	***eRR_ac***
RMSE	1.15	1.52	1.54	1.82	1.39	0.82

In Fig. 4 the correlation between values estimated using the *eRR_ac* estimator and values of RR calculated manually for measurements performed using the pressure belt is presented.

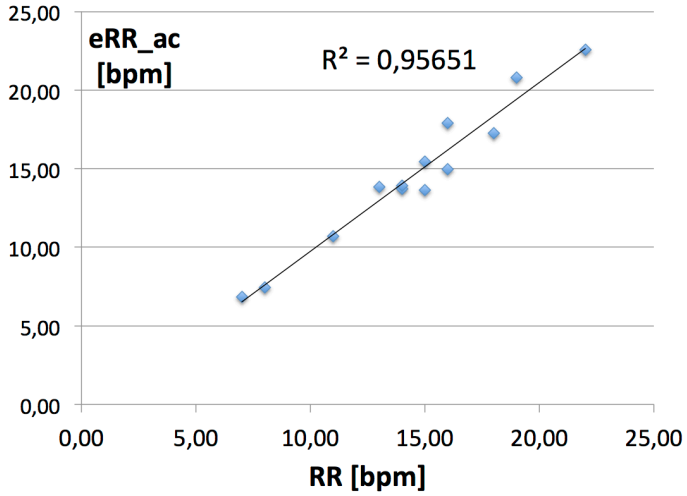

Fig. 4. *Correlation between values estimated using the eRR_ac estimator and values of RR calculated manually for measurements using pressure, chest belt*

4. Discussion and Conclusion

For the first experiment, pre-processed signals obtained using the belt and the thermal camera were stationary (verified with Augmented Dickey Fuller test) and highly coherent in the frequency range up to 1Hz (avg. integral of magnitude squared coherence estimate = 0.64±0.13). Results also showed that calculated respiration rates were almost identical. Only for 3 cases there are small differences for the zero-crossing method. There are also small differences between respiration rates calculated using *eRR_sp* and *eRR_zc* methods, partially due to limited spectral resolution (Fs/N, for small number of samples N). However, using the *eRR_sp* method the calculated values for both systems are exactly the same. Differences between calculated, normalized inspiration/expiration times periods are relatively high. However, high values of normalized differences are usually related to small offsets between detected times (samples) for related events. For example, if the inspiration period longs 1s (25 samples) then shift by 2 samples in inspiration start and stop events leads to 4/25=16% total difference. The respiration rate estimated by counting the inspiration events produced almost the same results as for the *eRR_zc* method (except it was not so sensitive for noise-related zero crossings).

The analysis performed for the second experiment (subjects speak) produced similar accuracy of the respiration rate estimation as for the experiment 1. However, inspiration events were not present so regularly and inspiration slopes were higher. Due to higher signal dynamics additional low-pass filtration was required. In this experiment results were compared to manually calculated *RR* values for measurements performed with the pressure belt. It is interesting to observe that the RMSE values are practically in the same range for both methods, i.e. for the belt and for the thermal camera. However, the best estimator in this experiment was the estimator based on autocorrelation function. This could be expected as the accuracy of the *eRR_sp* estimator highly depends on the frequency resolution in the frequency domain, which is limited by small number of samples. This is because the objective for this work was to analyze data in short time windows, so the healthcare professional could obtain first estimates of RR without long delay. Additionally, if the acquisition time is shorter then (usually) there are smaller artifacts related to patient movements. Reduction of such artifacts could be partially performed using automatic detection of the nostril region, which is a subject of our actual research [21][22].

Finally, it can be concluded that respiration rate and some respiration rhythm patterns (regularity, short-time variability, slopes, etc., when subject does not speak) can be reliable calculated using portable thermal camera for relatively short measurements. Respiration rate can be also reliable estimated for situations when subject speaks. This is very important since this enables to analyze how subjects control their breathing activities during speech. Additionally, remote methods for the estimation of respiration parameters are potentially more objective since a patient is not focusing on breathing activities but on other actions (i.e. on answering the questions during the interview).

REFERENCES

[1] MedicineNet.Com, Webster's New World Medical Dictionary, 3rd Edition, Wiley Publishing, Inc., Hoboken, New Jersey, 2008.
[2] Smith I, Mackay J, Fahrid N, Krucheck D. Respiratory rate measurement: a comparison of methods, British Journal of Healthcare Assistants. 05(01): 18-23, 2011.
[3] Neuman MI, Monuteaux MC, Scully KJ, Bachur RG. Prediction of pneumonia in a pediatric emergency department. *Pediatrics,*128:246-253, 2011.
[4] Bonita R, Beaglehole R, Kjellstrom T. Basic Epidemiology, 2nd edition, WHO, 2006.
[5] Nijman R G, Thompson M, van Veen M, Perera R, Moll H A, Oostenbrink R et al. Derivation and validation of age and temperature specific reference values and centile charts to predict lower respiratory tract infection in children with fever: prospective observational study *BMJ*; 345 :e4224, 2012.
[6] Cretikos MA, Bellomo R, Hillman K, Chen J, Finfer S, Flabouris A. Respiratory rate: the neglected vital sign, Medical Journal of Australia; 188: 657–659, 2008.
[7] Brouillette RT, Morrow AS, Weese-Mayer DE, Hunt CE. Comparison of respiratory inductive plethysmograpy and thoracic impedance for apnea; *The Journal of Pediatrics*, 111(3):377-383, 1987
[8] Anaxsys Technology Ltd, RespiR8, http://www.respir8.com/about_respiR8.html, 2011.
[9] Macknet MR, Kimball-Jones PL, Applegate RL, Martin RD, Allard MW. Accuracy and tolerance of a novel bioacoustic respiratory sensor in pediatric patients; *Anesthesiology.* A84, 2007.
[10] Hernandez J, McDuff D, Picard RW. Biowatch: Estimation of heart and breathing rates from wrist motions. 9th *PervasiveHealth Conference*, 167-176, Istanbul, 2015.
[11] Standards of Practice Committe of the American Sleep Disorders Association, Practice parameters for the indications for polysomnography and related procedures, *Sleep*, 20: 406–422, 1997.
[12] Przystup P, Bujnowski A, Ruminski J, Wtorek J. A multisensor detector of a sleep apnea for using at home, The 6th HSI Conference, IEEE Xplore, pp. 513-517, 2013.
[13] Bernal EA, Mestha LK, Shilla E. Non contact monitoring of respiratory function via depth sensing, *Biomedical and Health Informatics Conference (BHI), IEEE Xplore,* pp. 101-104, 2014.
[14] Ruminski J, Nowakowski A, Kaczmarek M, Hryciuk M. Model-based parametric images in dynamic thermography, Polish Journal of Med. Physics and Engineering, 6(3): 159-165, 2000.

[15] Ruminski J, Kaczmarek M, Renkielska A, Nowakowski A. Thermal parametric imaging in the evaluation of skin burn depth, IEEE Trans. on Biomedical Engineering, 54(2):303-312, 2007.
[16] Fei J, Zhu Z, Pavlidis I. Imaging breathing rate in the CO2 absorption band, Proc. of the 27th Annual Int. Conf. of the IEEE Engineering in Medicine and Biology Society, September 1-4, 2005.
[17] Murthy R, Pavlidis I. Non-contact monitoring of respiratory function using infrared imaging. IEEE Engineering in Medicine and Biology Magazine; 25: 57-68, 2006
[18] Murthy JN, van Jaarsveld J, Fei J, Pavlidis I, Harrykissoon RI, Lucke JF, Faiz S, Castriotta RJ. Thermal infrared imaging: A novel method to monitor airflow during polysomnography. SLEEP, 32:1521-1527, 2009.
[19] Fei J, Pavlidis I. Thermistor at a distance: unobtrusive measurement of breathing. IEEE Trans Biomed Eng, 57(4):988-998, 2010.
[20] Abbas AK, Heimann K, Jergus K, Orlikowsky T, Leonhardt S. BioMedical Engineering OnLine, 10(93):1-17, 2011.
[21] Kwasniewska A., Ruminski J., Face detection in image sequences using a portable thermal camera, Proc. Of the 13th Quantitative Infrared Thermography Conference, Gdansk 2016.
[22] Kwasniewska A., Ruminski J., Real-time facial feature tracking in poor quality thermal imagery, 9th International Conference on Human System Interaction, IEEE, eXplore, 2016.